

Biological approach to synthesize TiO_2 nanoparticles using *Staphylococcus aureus* for antibacterial and anti-biofilm applications

Abstract

Nano-sized materials have been an important tool in basic and applied sciences. A novel, low cost, green and reproducible bacteria, *Staphylococcus aureus* mediated biosynthesis of titanium dioxide nanoparticles (TiO_2 NPs) was reported in the present study. Initial conformational studies were done using UV-visible spectroscopy and confirmed the synthesis of TiO_2 NPs in the broth. The detailed characterization of the TiO_2 NPs was carried out using SEM, XRD, FTIR and Raman spectroscopy. From the SEM, it was confirmed that the sample showed the NPs were smooth and spherical with an average diameter of about 20nm. From FTIR analysis, it was confirmed that the TiO_2 nanoparticles are crystalline in nature, which was confirmed by the FTIR peak at 518cm^{-1} corresponds to the TiO_2 vibration present in a crystalline structure. Additionally, the synthesized NPs were also characterized by Transmission Electron Microscopy (TEM) and Particle size analyzer. This study was aimed to determine the antibacterial and antibiofilm activity of Titanium oxide nanoparticles against both Gram-positive and Gram-negative bacterial species and significant positive results against *Bacillus subtilis* and *Escherichia coli* were observed.

Keywords: *Staphylococcus aureus*, titanium dioxide nanoparticles, antibacterial, antibiofilm

Volume 8 Issue 1 - 2020

Kajal S Landage,¹ Gajanan K Arbade,² Pawan Khanna,¹ Chetan J Bhongale¹

¹Department of Applied Chemistry, Defence Institute of Advanced Technology, India

²Department of Materials Engineering, Defence Institute of Advanced Technology, India

Correspondence: Kajal S Landage, Department of Applied Chemistry, Defence Institute of Advanced Technology, Girinagar, Pune-411025, India, Email 2knawk@gmail.com

Received: January 02, 2020 | **Published:** February 04, 2020

Introduction

Nanoparticles are quite often employed in the field of nanotechnology which has become the current research trend. However, chemical compositions, sizes and high monodispersity are one of the challenging issues in nanotechnology for the development of reliable protocols for the synthesis of nanoparticles.^{1,2} An important area of research in nanoscience deals with the synthesis of nanometer-sized materials of different morphologies, sizes and with mono dispersion.^{3,4} In modern nanotechnology, the interaction between inorganic nanoparticles and biological structures are one of the most exciting areas of research. But there is a need to develop an eco-friendly approach for nanomaterials synthesis from the point of view of environmental health and social aspects. Different microorganisms produce inorganic materials either intracellularly or extracellularly.^{5,6} Nanotechnology deals with materials having the size in the range of 100 nm. NPs show different properties and depending on the properties it has been used in different domains for various applications.⁶⁻¹⁰

The microorganisms are used as possible “nano factories” for development of clean, nontoxic and environmentally friendly methods for producing nanoparticles. Various chemical and physical methods are employed for the synthesis of nanoparticles.¹¹⁻¹³ The synthesis of nanoparticles may cause adverse environmental and health effects.^{13,14} There are different methods for the synthesis of TiO_2 NPs such as sol-gel, hydrothermal, fungal mediated biosynthesis etc. The production of silver nanoparticles within the periplasmic surface of *Pseudomonas stutzeri*, the formation of gold nanoparticles using *Salmonella typhi*.¹⁵⁻¹⁸ and *C. limone* were demonstrated practically using the above technique.^{19,20} Biological synthesis are beneficial when compared to synthetic methods as biological methods are more eco-friendly.²⁰⁻²² The biological method for nanoparticle synthesis is simple, eco-friendly and allows for getting controlled size nanoparticles which can be used as catalysts with specific composition, which is not possible by classical methods. Applications in sensors and medicine

are envisaged and the nanoparticles synthesized by using bacterial strains can be further used for biomedical applications.

Titanium, for its weight property and strength, has been used in various industries for a variety of applications. It is lighter than steel with good mechanical strength and twice as strong as aluminium.^{19,20,23} In the present study, the above aspects have been considered, in order to develop an ecofriendly biotechnological approach for the production of TiO_2 NPs. It has also been found in the literature that *Lactobacillus* has been used for synthesis similar synthesis.²⁴ Due to its properties among other oxide semiconductors, TiO_2 has been more in use in a variety of industrial applications.²⁵ TiO_2 is a great material for photocatalysis and development of various biomaterials.²⁶ The biocompatibility property of titania allows its use in bone tissue engineering for the regeneration and healing of damaged bone.²⁷⁻²⁹ TiO_2 is an efficient catalyst, can be used further for the removal of numerous environmental pollutants and it has been demonstrated for water and surface cleaning.^{11,29,30} In the present study, we have synthesized TiO_2 NPs by using *S. aureus*. The antimicrobial and anti-Biofilm property of TiO_2 NPs was utilized here for the biomedical application. A typical scheme of the work is represented in Figure 1.

Materials and methods

Materials

Titanium tetraisopropoxide (TIP) with an average molecular weight 284.25g/mol and ethanol were purchased from Sigma Aldrich, India. Nutrient agar, Nutrient broth and bacteriological Agar powder were purchased from Himedia, India. All the chemicals, solvents and reagents used in the study were of analytical grade and used without any further purification. The bacterial strains (*Escherichia Coli*, *Bacillus subtilis* and *Staphylococcus aureus*) used during the present studies were obtained from the National Chemical Laboratory, Commercial Unit, India.

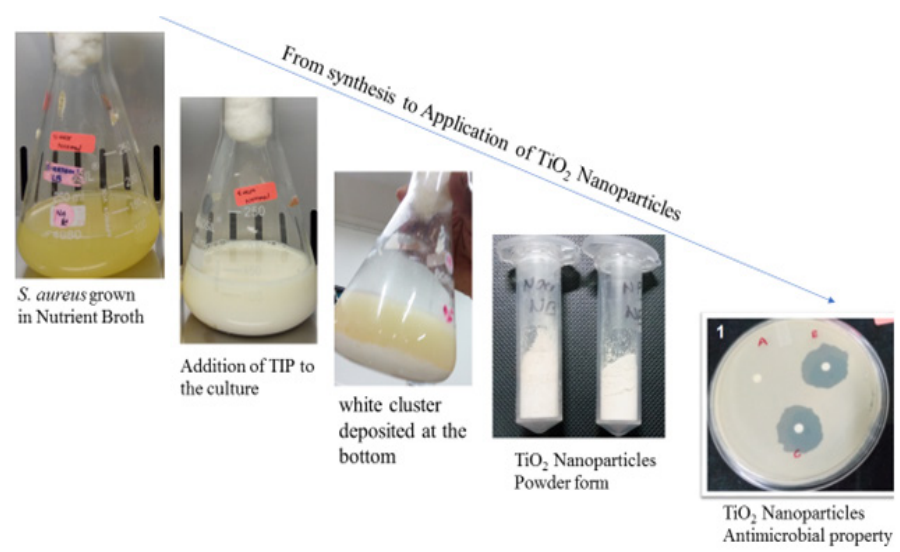


Figure 1 Schematic representation of the present study.

Synthesis of TiO_2 nanoparticles using *S. aureus*

S. aureus cells were allowed to grow as a suspension culture in 100ml sterile nutrient broth medium for 36h. This culture was treated as source culture. 25ml of source culture was taken and diluted four times by adding 75ml of sterile nutrient broth medium. This diluted culture solution was again allowed to grow for another 24h. 20 ml 0.0025M $[\text{Ti}(\text{OH})_2]$ titanium tetraisopropoxide was mixed to the broth culture and kept in a steam bath for ~20min at 60°C . As white deposition was observed bottom of the flask, indicating transformation initiation. The broth culture containing *S. aureus* was incubated at room temperature. After 12-48 h, the broth culture was observed for distinctly markable coalescent white cluster deposited at the bottom confirming the synthesis of TiO_2 NPs.

Characterization of TiO_2 nanoparticles

The Synthesis of TiO_2 nanoparticles in the broth medium was confirmed by taking UV absorbance by Biospectrotometer (Eppendorf, Germany). The X-ray diffraction (XRD) patterns of the samples were measured by using X-ray diffractometer with $\text{Cu-K}\alpha$ radiation. The crystalline nature and average crystallite size of the TiO_2 nanoparticles were recorded using X-ray diffraction (XRD) (Bruker, Germany) with $\text{CuK}\alpha$ radiation (1.5406 \AA) in the 2θ scan range of 10 – 90° . To investigate the morphology and diameter of the nanoparticles SEM was conducted using FE-SEM (ZEISS, Germany). FTIR spectrum of TiO_2 nanoparticles was recorded on Fourier Transform Infrared spectrophotometer (Bruker, Germany) in the region of 4000 to 500 cm^{-1} . The surface morphology of the NPS was observed using SEM and AFM. While the average diameters and size distributions of TiO_2 NPs were calculated by counting over 50 particles from the SEM Micrographs by ImageJ software. The excitation and photoluminescence (PL) spectra of the sample were recorded on a spectrophotometer (Agilent Technologies) in the range of 250nm to 800nm with an excitation wavelength of 320nm . The average particle size distribution was carried out using Particle size analyzer. Raman spectra were recorded using EZ Raman spectrometer in the range 4000 to 400cm^{-1} Where emitted wavelength is 780nm . The

photocatalytic activities were done under UV applying 254nm and 365nm irradiation.

Antibacterial properties of TiO_2 nanoparticles

The antibacterial activity of TiO_2 NPs was studied by disc diffusion method.³¹ The desired concentrations of TiO_2 were prepared by dissolving the appropriate amount TiO_2 NPs powder and dissolved in DI water. The Whatman filter paper discs were prepared of 3mm diameter, sterilized and then added to the TiO_2 solution. Simultaneously, the nutrient agar plates were prepared seeded with the bacterial cultures and allowed to grow for overnight at 37°C along with the discs loaded with TiO_2 NPs. After incubation, the plates were observed for the inhibition zones and recorded.

Effect of TiO_2 nanoparticles on bacterial biofilm formation by tube method

The assessment of biofilm formation qualitatively was determined by tube method. Simply, Brain Heart Infusion Broth (BHI) + sucrose (2%) + 0.5ml TI-NP (15mg/ml) was used for bacterial inoculation. BHI/sucrose inoculated plate was used as a control. Both the plates were incubated at 37°C for 24 h in bacteriological incubator. To study the biofilm-forming potential the glass tubes were decanted and washed with distilled water and dried tubes were stained with crystal violet (0.1%). Excess stain was removed and tubes were washed with de-ionized water. The biofilm formation was observed by drying tubes in an inverted position. Biofilm formation was considered positive when a visible film lined the wall and bottom of the tube. Ring formation at the liquid interface was not indicative of biofilm formation.

Results and discussion

UV-visible spectra analysis

In order to confirm the synthesis of TiO_2 NPs, the UV absorption was checked. Figure 2 shows the UV-Visible spectra for the TiO_2 nanoparticles. The UV spectra show a distinct absorption peak confirming the anatase phase of nano- TiO_2 . The cut off wavelength of TiO_2 nanoparticles was observed at 324nm . It is matching with the

previous studies of our research group.³² The band gap of TiO_2 was calculated using equation 1.

$$E = \frac{hc}{\lambda} \text{ (Equation 1)}$$

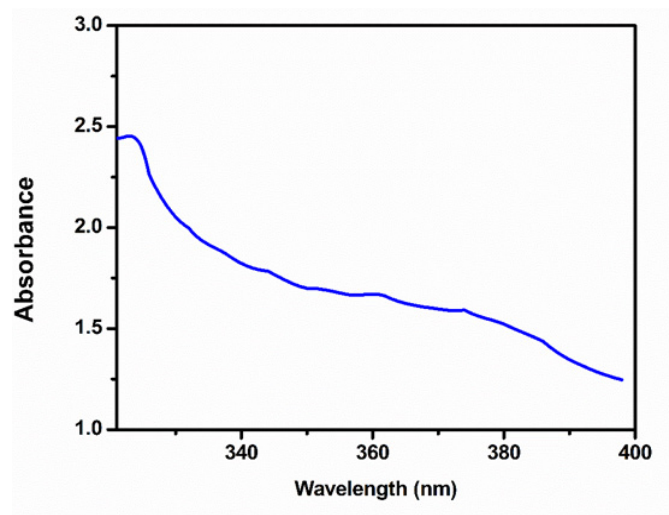


Figure 2 UV absorbance of TiO_2 NPs synthesized by *S. aureus*.

Where, h =Plank constant (6.626×10^{-34} Joules sec), c =Speed of the light (3.0×10^8 meter/sec), k =cut off wavelength (410.57×10^{-9} meters). The band gap value of the TiO_2 was found to be 3.88 eV. In the present study, the bandgap value (3.88 eV), which is close to those reported for the anatase TiO_2 nanoparticles.

Scanning electron microscopy (SEM): The surface morphology, shape and size of NPs were analyzed by SEM. Figure 3 shows SEM images of TiO_2 nanoparticles synthesized by using a bacterial strain *S. aureus*. The nanoparticles were spherical, oval in shape, smooth surface and having an average diameter of around 20 nm.

Particle size analyzer: Figure 4 represents the particle size distribution of TiO_2 NPs. The particle size of the nanoparticle ranges in size from 10 to 30 nm which is a good agreement with the SEM results. The uneven distribution of NPs can be clearly observed.

FTIR analysis: Fourier transform infrared spectroscopic analysis was performed to apprehend the interaction of NPs with capping agents. The FTIR spectra of TiO_2 nanoparticles show the presence of broadband at $3000\text{--}3500\text{cm}^{-1}$ corresponds to stretching vibration of terminating hydroxyl groups in samples. The spectra of TiO_2 NPs exhibited prominent peaks at $2923, 2856, 1649, 1545, 1450, 1393, 1234, 1069$ and 679cm^{-1} (Figure 5(a)). The main peaks due to C–H symmetric and asymmetric stretching, C=O stretching and C–O stretching frequencies were observed near 2923cm^{-1} , 1638cm^{-1} , 1069cm^{-1} respectively. The Peaks at $1450, 1393$ and 1164 were assigned for bending vibrations of primary and secondary amines. The peak at 2923cm^{-1} corresponds to carboxylic groups. The peak 2856cm^{-1} corresponds to C–H stretch, 1649cm^{-1} corresponds to C=O stretch of amines. The peaks at $2923, 1649$ and 679cm^{-1} are observed in the spectra due to the biogenic substances (lipids and proteins) associated with the synthesis of TiO_2 nanoparticles. In addition, peak at the 679cm^{-1} corresponds to metal binding to carboxylic groups proposed that the proteins could bind with nanoparticles through the free amines groups or crystalline residues in the proteins, might help in the nucleation of nanoparticles formation.³

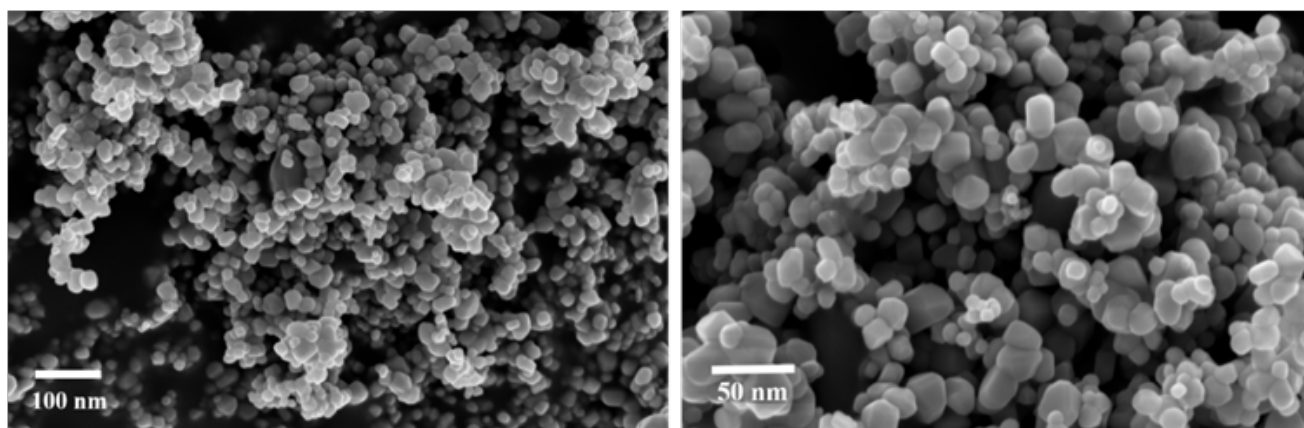


Figure 3 Scanning Electron microscope images of TiO_2 nanoparticles.

Photoluminescence studies: To understand the luminescence properties of synthesized nanoparticles, the photoluminescence analysis has been employed. It was observed that the emission band for NPs was about 390 nm. The light-emitting property of nano-titania may rise due to the existence of surface plasmons. Figure 5(b) shows a Stokes shift of 70–76 nm with reference to absorbance band ($\sim 3.88\text{ eV}$, 324 nm). Therefore, rules out the emission in the visible light range due to the absence of free Ti–OH states.³²

Atomic force microscopy: The AFM was performed to have more insight into the topological map of the surface and agglomeration of TiO_2 NPs. The AFM obviously depicts the formation of the rutile and anatase forms in the TiO_2 NPs, and the surface morphology of the particle which was uneven due to the presence of some aggregate and individual particles. AFM offered a three-dimensional visualization of TiO_2 . The strong crystalline nature can be observed in the form of diagonal formations with ridges (Figure 6). By means of AFM no linear trend in roughness was observed, but it is proved that the

highest TiO_2 concentration results in the formation of a smoother layer. In AFM analysis it was observed that the TiO_2 NPs were in the size of 10-20nm which was in good agreement with SEM and XRD data.^{18,29,33}

XRD analysis: The crystal phase of the TiO_2 was confirmed using XRD. The XRD patterns of the NPs synthesized by using the bacterium *Staphylococcus aureus* is shown in Figure 7(a) The appearance of sharp diffraction patterns designates the small size, crystalline and high purity of the synthesized sample.³⁴

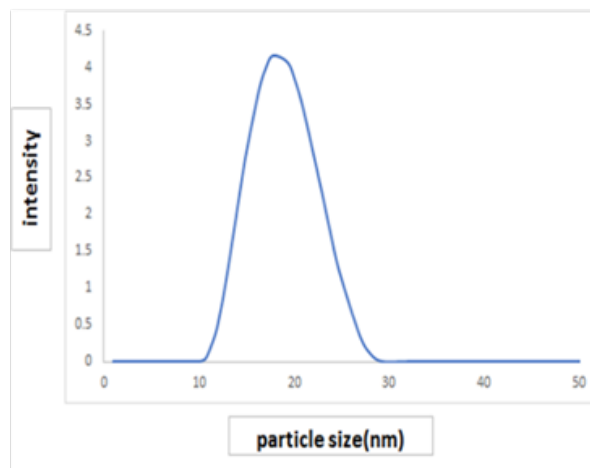
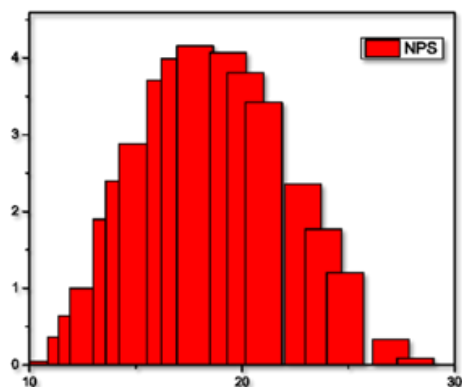


Figure 4 Particle size of TiO_2 NPs.

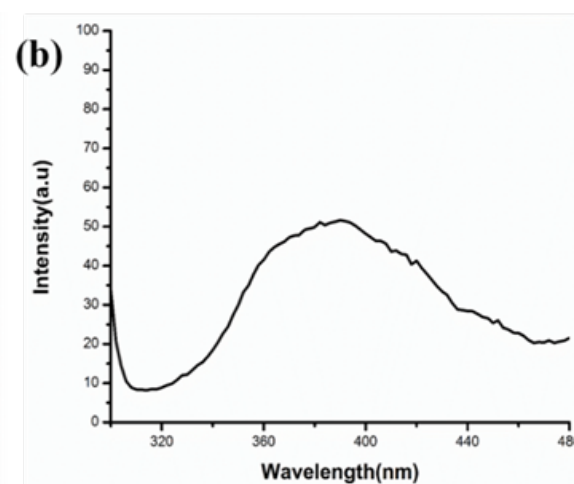
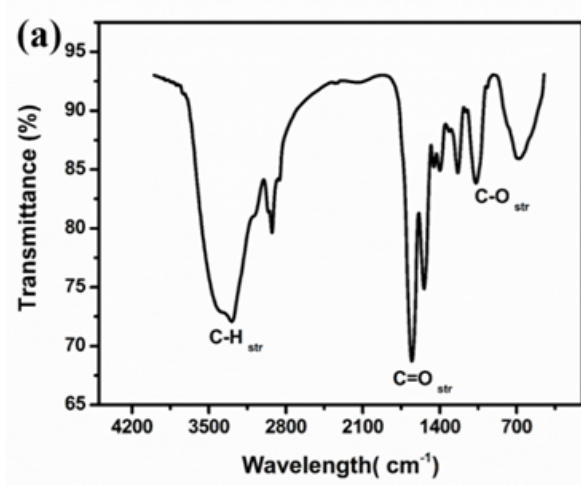


Figure 5 (a) FTIR analysis of TiO_2 NPs synthesized by using TiO_2 NPs and (b) Photoluminescence spectra of TiO_2 NPs synthesized by *S. aureus*.

The line broadening of the diffraction peaks shows that materials were in the nanometer range. The diffraction patterns showed that the anatase phase ($a=3.782 \text{ \AA}$, JCPDS no: 84-1286) was formed.³⁵ The prominent peaks obtained in the XRD pattern of the bio-mediated synthesis of TiO_2 nanoparticle after removing organic impurities by heating. The peak signals at (101), (103), (004), (112), (200), (105), (211), (204), (220), (215) and (224) planes confirm that the formation of anatase crystal phase mostly, which coincides with JCPD 89-4921 standard.¹⁷ Average particle size was calculated using Scherrer's equation (equation 2):

$$\tau = \frac{k\lambda}{\beta \cos \theta} \quad (\text{Equation 2})$$

Where λ is the X-ray wavelength, typically 1.54 \AA , K is the shape

factor, (0.9) , β is the line broadening at half the maximum intensity (FWHM) in radians, θ is the Bragg angle, τ is the particle size. The size of the bio-mediated TiO_2 particle was found between 17.01-18.19nm. The 2θ at peak 25.29° confirms the TiO_2 anatase structure. Strong diffraction peaks at 25° and 48° indicating TiO_2 in the anatase phase. There were many other diffraction peaks found in the sample that might because of bacterial cell proteins. The 2θ peaks at 25.29° and 48.21° confirm its anatase structure.

Raman analysis: The structural properties of the TiO_2 NPs were further investigated by Raman spectroscopy. Figure 7(b) represent the Raman spectra for TiO_2 nanoparticles. The spectrum was typical of the anatase TiO_2 phase confirms the phase obtained from XRD. According to factor group analysis, anatase has six Raman active modes ($A_{1g} + 2B_{1g} + 3E_g$).³⁶ The Raman spectrum of an anatase single crystal has

been investigated by Ohsaka and others³⁶ who concluded that the six distinct active modes appeared at 136cm^{-1} (E_g), 190cm^{-1} (E_g), 388cm^{-1} (B_{1g}), 504cm^{-1} (A_{1g}), 516cm^{-1} (B_{1g}) and 630cm^{-1} (E_g). The Raman spectra indicate that the anatase shell was crystallized; a Raman shift at 136cm^{-1} can be attributed to the dominating E_g vibrational mode in anatase TiO_2 . The main features of the spectra of the sample are very

similar to those of the reference TiO_2 , which means that the anatase phases of the nanoparticles of samples possess a certain degree of long-range order. Comparing the obtained Raman spectra with the available literature.^{37,38} It is clear that the Raman bands shift towards higher wave number and their intensities relatively decrease as the particle size decreases.

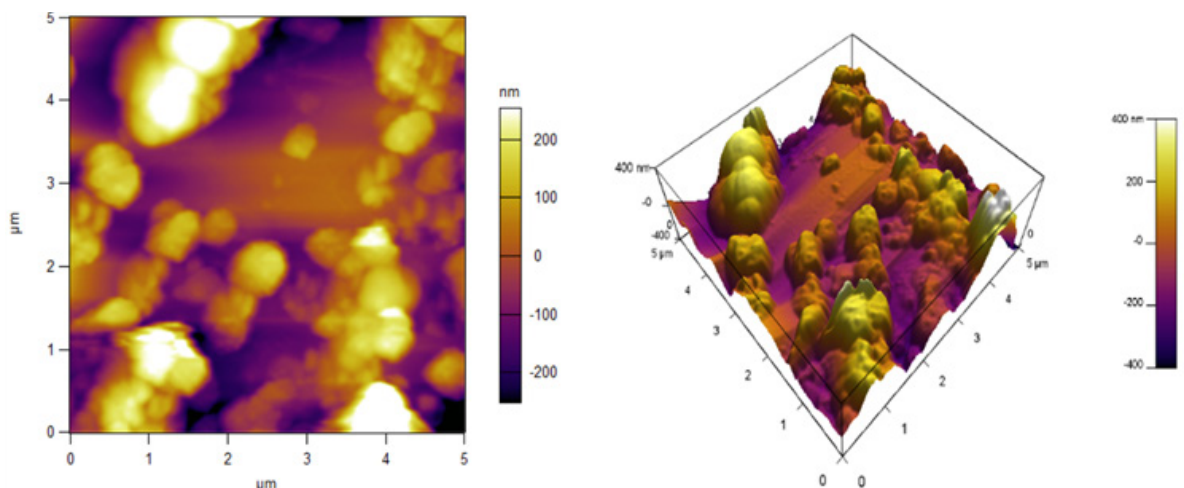


Figure 6 Atomic Force Microscopy of TiO_2 NPs synthesized by *S. aureus*.

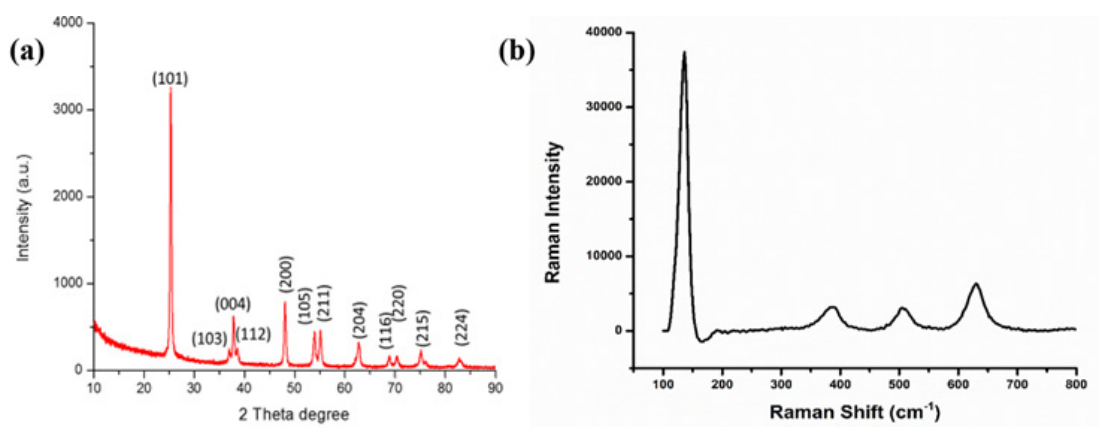


Figure 7 (a) XRD pattern of TiO_2 NPs and (b) Raman spectra of TiO_2 NPs.

Transmission electron microscopy (TEM): It is shown that the as-prepared powder was completely crystalline and entirely consists of anatase phase. Due to the relatively poor contrast in the micrograph, it is difficult to exactly measure the size of the primary spherical particles accurately. From the micrograph, their diameter is estimated to be below 20nm, which is in good agreement with the XRD results. The first four rings are assigned to the (101), (004), (200), (005) reflections of the anatase phase.

Figure 8 shows the TEM image of TiO_2 nanoparticles. It is elucidated from the figure that the TiO_2 NPs were agglomerated; mostly spherical in shape and size of particles was in the range of 10–20 nm. This result supports our XRD data in determining the particles size, which coincides with a TEM image. The lattice fringes calculated as 0.327nm which are in good agreement with the previous reports for anatase phase titania NPs respectively.^{17,32,39}

Antimicrobial activity of TiO_2 NPs: Figure 9 shows the antibacterial activity of TiO_2 nanoparticles, it was carried out by disc diffusion method against two bacterial strains viz. *Escherichia coli* and *Bacillus subtilis*. The formation of inhibition zones around the TiO_2 nanoparticles integrated discs clearly shows the sensitivity of the bacterial species to TiO_2 nanoparticles. The diameter of the inhibition zone was measured for each bacterium, shown in Table 1. The differential sensitivity of Gram-negative and Gram-positive bacteria towards nanoparticles may be depends upon their cell outer layer attribute and their interaction with the charged TiO_2 nanoparticles. It was observed that Gram-negative bacteria are more sensitive than Gram-positive bacteria. This property of TiO_2 NPs can be utilized in coating the medical devices like catheters to avoid the opportunistic pathogenic infection.

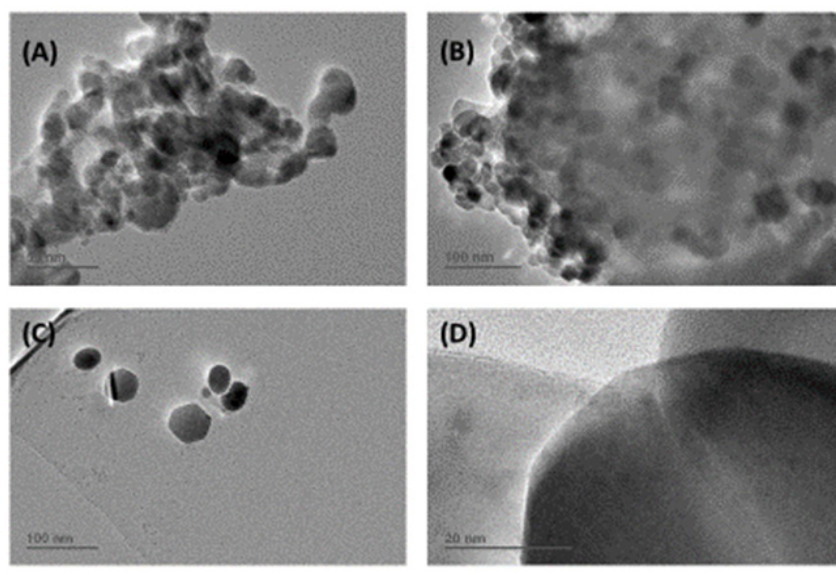


Figure 8 Transmission Electron Micrographs TiO_2 NPs (A)-(D) at different resolutions.

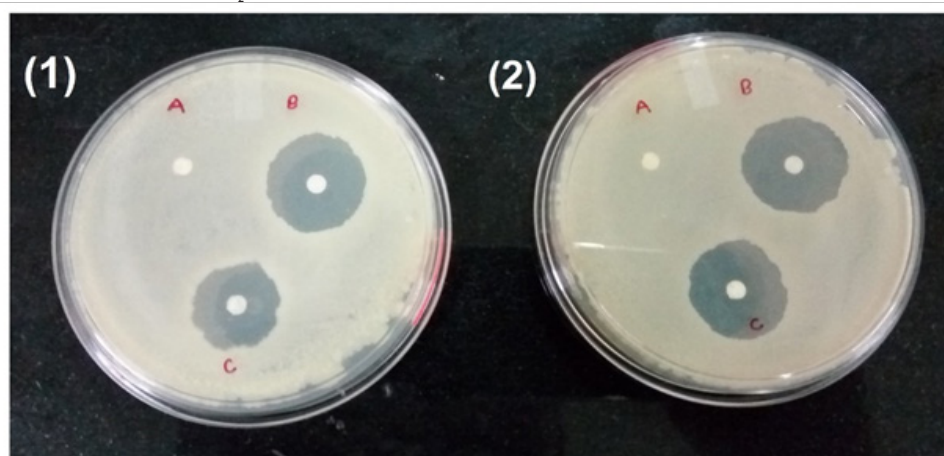


Figure 9 Antibacterial activity of TiO_2 NPs (1) against *B. subtilis* (A) Control (B) 15mg/mL TiO_2 NPs (C) 10mg/mL TiO_2 NPs (2). Against *E. coli* (A) Control (B) 15mg/mL TiO_2 NPs (C) 10mg/mL TiO_2 NPs.

Table 1 Zone of inhibition against bacterial strains by TiO_2 NPs

S. No	Bacterial Strain	Zone of Inhibition (mm)
		TiO_2 NPs
1	<i>E. coli</i>	14
2	<i>B. subtilis</i>	9

Table 2 Effect of TiO_2 nanoparticles on bacterial biofilm formation

S. No	Bacterial strain	Biofilm formation	
		Control (without NPs)	In presence of TiO_2 NPs
1	<i>E. coli</i>	++++	++
2	<i>B. subtilis</i>	+++++	+++

Representation in table: (++) moderate (+++++) strong

Effect of TiO_2 NPs on bacterial biofilm formation

Biofilm forming potential of bacterium increases its pathogenicity and increases the chances of opportunistic infections, which are extremely difficult to eliminate. Biofilm forming strains show resistance to antibiotics. The ability of a bacterium to form a biofilm, they are found as a common contaminant in medical devices like catheters. The immune compressive host is very prone to the infections by such pathogen. TiO_2 NPs moving beyond viability and growth; a functional assessment performed examining specific function. The biofilm formation is a common phenomenon in bacteria especially has a role in quorum sensing etc. A comparative study was done to study the biofilm formation in *Bacillus subtilis* and *E. coli* with and without nanoparticles. As mentioned in Table 2, biofilm formation was reduced approximately by 40-50% in the presence of TiO_2 nanoparticles for both Gram-positive and Gram-negative bacterial strains.

Conclusion

In conclusion, the present biotechnological method is capable of producing TiO_2 nanoparticles with significant antimicrobial activity. We have used an efficient and eco-friendly approach for rapid synthesis of TiO_2 nanoparticles. The bacterium mediated TiO_2 synthesis exhibits a greater advantage over other conventional techniques in 12-20h. The physicochemical properties of synthesized TiO_2 -NPs were investigated by UV-Vis spectroscopy, XRD, TEM, FTIR, Raman, AFM, SEM, PL, and TEM, indicating that TiO_2 -NPs crystallize in the anatase phase with smaller size range and it provides a pure form of NPs. The synthesis of TiO_2 nanoparticles was confirmed by a colour change of the liquid medium from yellow to intense dark white in colour and it exhibited at maximum absorbance at 324nm play a prominent role in reduction TIP to TiO_2 nanoparticles. The XRD studies showed the crystalline nature of nanoparticles. The possibility of protein as stabilizing material in TiO_2 nanoparticles is exposed by the FTIR analysis. Nanoparticles with smooth surface morphology and average particle size about 20-30nm were conformed and the anatase TiO_2 NPs were formed with the size in the range of 10-30nm that was confirmed by AFM analyses too. These nanoparticles biosynthesis from *S. aureus* showed excellent antibacterial, antibiofilm, properties against various bacterial strains including *E. coli*, and *Bacillus Subtilis*.

These nanoparticles can be further used for the coating purposes in medical devices (e.g. catheters) to control the concerned bacterial infections. The suitability of the TiO_2 nanoparticles is because of anti-biofilm activity rather than antibacterial activity, as the pathogenic bacteria grow in/on medical devices by producing biofilm. Presence of biofilm in bacterial colonies shows more resistance towards regular antibiotics and disinfectants used in the hospitals to clean the medical devices such as catheters, pipes used during kidney, other urinary tract infections and ineffective function etc. biomedical applications.

Acknowledgments

Authors KSL and GKA thank AICTE and Defence Institute of Advanced Technology, Pune, India for providing research Fellowship respectively.

Conflicts of interest

Authors declare that there is no conflicts of interest.

References

- Jha AK, Prasad K, Kulkarni AR. Synthesis of TiO_2 Nanoparticles Using Microorganisms. *Colloids Surfaces B Biointerfaces*. 2009;71(2):226–229.

- Mukherjee P, Ahmad A, Mandal D, et al. Fungus-Mediated Synthesis of Silver Nanoparticles and Their Immobilization in the Mycelial Matrix: A Novel Biological Approach to Nanoparticle Synthesis. *Nano Lett*. 2001;1(10):515–519.
- Mandal D, Bolander ME, Mukhopadhyay D, et al. The Use of Microorganisms for the Formation of Metal Nanoparticles and Their Application. *Appl Microbiol Biotechnol*. 2006;69(5):485–492.
- Yedurkar SM, Maurya CB, Mahanwar PA. Synthesis of Nanoparticles by Green Chemistry Process and Their Application in Surface Coatings: A Review. *Arch Appl Sci Res*. 2016;8(5):55–69.
- Bhattacharya D, Gupta RK. Nanotechnology and Potential of Microorganisms. *Crit Rev Biotechnol*. 2005;25(4):199–204.
- Iravani S. Bacteria in Nanoparticle Synthesis: Current Status and Future Prospects. *Int Sch Res Not*. 2014;2014:1–18.
- Goodsell DS. *Bionanotechnology Today*; 2004.
- Salata OV. Applications of nanoparticles in biology and medicine. *J Nanobiotechnology*. 2004;2(3):1–6.
- Ahmad A, Mukherjee P, Senapati S, et al. Extracellular Biosynthesis of Silver Nanoparticles Using the Fungus *Fusarium Oxysporum*. *Colloids Surfaces B Biointerfaces*. 2003;28(4):313–318.
- Marrian CRK. Investing in Nanotechnology. *Int Microprocess Nanotechnol Conf*. 2001;21(10):72.
- Sun Y, Mayers B, Xia Y. Transformation of Silver Nanospheres into Nanobelts and Triangular Nanoplates through a Thermal Process. *Nano Lett*. 2003;3(5):675–679.
- Sadasivan S, Khushalani D, Mann S. Synthesis of Calcium Phosphate Nanofilaments in Reverse Micelles. *Chem Mater*. 2005;17(10):2765–2770.
- Ali FA. Effect of titanium nanoparticles biosynthesis by *Lactobacillus crispatus* on urease, hemolysin & biofilm forming by some bacteria causing recurrent UTI in Iraqi women Kawther Hkeem Ibrahim. *Eur Sci J*. 2014;10(9):324–338.
- Parashar UK, Saxena PS. Bioinspired Synthesis of Silver Nanoparticles. *J Nanomater*. 2009;4(1):159–166.
- Prathna TC, Chandrasekaran N, Raichur AM, et al. Biomimetic Synthesis of Silver Nanoparticles by Citrus Limon (Lemon) Aqueous Extract and Theoretical Prediction of Particle Size. *Colloids Surfaces B Biointerfaces*. 2011;82(1):152–159.
- Oza G, Pandey S, Mewada A, et al. Extracellular Biosynthesis of Gold Nanoparticles Using *Salmonella Typhi*. *Der Chem Sin*. 2012;3(5):1041–1046.
- Dhandapani P, Maruthamuthu S, Rajagopal G. Bio-Mediated Synthesis of TiO_2 Nanoparticles and Its Photocatalytic Effect on Aquatic Biofilm. *J Photochem Photobiol B Biol*. 2012;110:43–49.
- Velayutham K, Rahuman AA, Rajakumar G, et al. Evaluation of Catharanthus Roseus Leaf Extract-Mediated Biosynthesis of Titanium Dioxide Nanoparticles against *Hippobosca Maculata* and *Bovicola Ovis*. *Parasitol Res*. 2012;111(6):2329–2337.
- Tripathy A, Raichur AM, Chandrasekaran N, et al. Process Variables in Biomimetic Synthesis of Silver Nanoparticles by Aqueous Extract of *Azadirachta Indica* (Neem) Leaves. *J Nanoparticle Res*. 2010;12(1):237–246.
- Malarkodi C, Chitra K, Rajeshkumar S, et al. Novel Eco-Friendly Synthesis of Titanium Oxide Nanoparticles by Using *Planomicrobium Sp.* and Its Antimicrobial Evaluation. *Der Pharm*. 2013;4(3):59–66.
- Parashar V, Parashar R. Parthenium Leaf Extract Mediated Synthesis of Silver Nanoparticles: A Novel Approach towards Weed Utilization. *Dig J Nanomater Biostructures*. 2009;4(1):45–50.

22. Goud KA, Narendra JN, Nargund LVG, et al. Synthesis of Novel Benzothiazoles for Anti-Bacterial Activity. *Der Pharma Chem.* 2012;4(4):1408–1414.
23. Popescu M, Velea A, Lorinczi A. Biogenic production of nanoparticles. *Dig J Nanomater Biostructures.* 2010;5(4):1035–1040.
24. Klaus-Joerger T, Joerger R, Olsson E, et al. Bacteria as Workers in the Living Factory: Metal-Accumulating Bacteria and Their Potential for Materials Science. *Trends Biotechnol.* 2001;19(1):15–20.
25. Abdul J, Salman S, Ibrahim KH, et al. Effect of Culture Media on Biosynthesis of Titanium Dioxide Nanoparticles Using *Lactobacillus Crispatus* Material and Methods: Results and Discussion. *Int J Adv Res.* 2014;2(5):1014–1021.
26. Jayaseelan C, Rahuman AA, Roopan SM, et al. Biological Approach to Synthesize TiO_2 nanoparticles Using *Aeromonas Hydrophila* and Its Antibacterial Activity. *Spectrochim Acta-Part A Mol Biomol Spectrosc.* 2013;107:82–89.
27. Joerger R, Klaus T, Granqvist CG. Biologically Produced Silver - Carbon Composite Materials for Optically Functional Thin-Film Coatings. *Adv Mater.* 2000;12(6):407–409.
28. Tolles WM, Rath BB. Nanotechnology, a Stimulus for Innovation. *Curr Sci.* 2003;85(12):1746–1759.
29. Vishnu Kirthi A, Abdul Rahuman A, Rajakumar G, et al. Biosynthesis of Titanium Dioxide Nanoparticles Using Bacterium *Bacillus Subtilis*. *Mater Lett.* 2011;65(17–18):2745–2747.
30. Gélis C, Girard S, Mavon A, et al. Assessment of the Skin Photoprotective Capacities of an Organo-Mineral Broad-Spectrum Sunblock on Two Ex Vivo Skin Models. *Photodermatol Photoimmunol Photomed.* 2003;19(5):242–253.
31. Arbade GK, Jathar S, Tripathi V, et al. Antibacterial, Sustained Drug Release and Biocompatibility Studies of Electrospun Poly (ϵ -Caprolactone)/Chloramphenicol Blend Nanofiber Scaffolds. *Biomed Phys Eng Express.* 2018;4(4):045011.
32. Gautam A, Kshirsagar A, Biswas R, et al. Photodegradation of Organic Dyes Based on Anatase and Rutile TiO_2 Nanoparticles. *RSC Adv.* 2016;6(4):2746–2759.
33. Sunkar S, Nachiyar CV, Lerensha R, et al. Biogenesis of TiO_2 Nanoparticles Using Endophytic *Bacillus Cereus*. *J Nanoparticle Res.* 2014;16:2681.
34. Pan X, Medina-Ramirez I, Mernaugh R, et al. Nanocharacterization and Bactericidal Performance of Silver Modified Titania Photocatalyst. *Colloids Surfaces B Biointerfaces.* 2010;77(1):82–89.
35. Babitha S, Korrapati PS. Biosynthesis of Titanium Dioxide Nanoparticles Using a Probiotic from Coal Fly Ash Effluent. *Mater Res Bull.* 2013;48(11):4738–4742.
36. Ohsaka T. Temperature Dependence of the Raman Spectrum in Anatase TiO_2 . *J Phys Soc Japan.* 1980;48(5):1661–1668.
37. Choi HC, Jung YM, Kim SB. Size Effects in the Raman Spectra of TiO_2 Nanoparticles. *Vib Spectrosc.* 2005;37(1):33–38.
38. Ramimoghdam D, Bagheri S, Abd Hamid SB. Biotemplated Synthesis of Anatase Titanium Dioxide Nanoparticles via Lignocellulosic Waste Material. *Biomed Res Int.* 2014;2014:205636.
39. Mahata S, Mahato SS, Nandi MM, et al. Synthesis of TiO_2 Nanoparticles by Hydrolysis and Peptization of Titanium Isopropoxide Solution. *Funct Mater.* 2012;1461:225–228.